Available online at www.sciencedirect.com

SCIENCE DIRECT®

Biochimica et Biophysica Acta 1656 (2004) 88–95

BIOCHIMICA ET BIOPHYSICA ACTA
BBA

www.bba-direct.com

Thermoinactivaion analysis of vacuolar H^+-pyrophosphatase

Su J. Yang[a], Shih S. Jiang[b], Yi Y. Hsiao[c], Ru C. Van[c], Yih J. Pan[c], Rong L. Pan[c,*]

[a] *Department of Radiological Technology, Chungtai Institute of Health Sciences and Technology, Taichung 40605, Taiwan, ROC*
[b] *Division of Molecular and Genomic Medicine, National Health Research Institutes, Taipei 11529, Taiwan, ROC*
[c] *Department of Life Sciences and Institute of Bioinformatics and Structural Biology, College of Life Sciences, National Tsing Hua University, Hsin Chu 30043, Taiwan, ROC*

Received 17 October 2003; received in revised form 8 January 2004; accepted 3 February 2004

Available online 20 February 2004

Abstract

Vacuolar H^+-translocating pyrophosphatase (H^+-PPase; EC 3.6.1.1) catalyzes both the hydrolysis of PP_i and the electrogenic translocation of proton from the cytosol to the lumen of the vacuole. Vacuolar H^+-PPase, purified from etiolated hypocotyls of mung bean (*Vigna radiata* L.), is a homodimer with a molecular mass of 145 kDa. To investigate the relationship between structure and function of this H^+-translocating enzyme, thermoinactivation analysis was employed. Thermoinactivation studies suggested that vacuolar H^+-PPase consists of two distinct states upon heat treatment and exhibited different transition temperatures in the presence and absence of ligands (substrate and inhibitors). Substrate protection of H^+-PPase stabilizes enzyme structure by increasing activation energy from 54.9 to 70.2 kJ/mol. We believe that the conformation of this enzyme was altered in the presence of substrate to protect against the thermoinactivation. In contrast, the modification of H^+-PPase by inhibitor (fluorescein 5′-isothiocyanate; FITC) augmented the inactivation by heat treatment. The native, substrate-bound, and FITC-labeled vacuolar H^+-PPases possess probably distinct conformation and show different modes of susceptibility to thermoinactivation. Our results also indicate that the structure of one subunit of this homodimer exerts long distance effect on the other, suggesting a specific subunit–subunit interaction in vacuolar H^+-PPase. A working model was proposed to interpret the relationship of the structure and function of vacuolar H^+-PPase.

Keywords: Tonoplast; Vacuolar H^+-pyrophosphatase; Thermoinactivation; Subunit interaction; Circular dichroism; Differential scanning calorimetry

1. Introduction

A characteristic feature of plant vacuoles is the existence of two parallel proton-pumping systems, a vacuolar H^+-ATPase (EC 3.6.1.3) and a vacuolar H^+-pyrophosphatase (H^+-PPase; EC 3.6.1.1). Vacuolar H^+-ATPase is an enzyme common to all eukaryotes, while vacuolar H^+-PPase is found primarily in higher plants, some alga, protozoa, bacteria, and archaebacteria [1,2]. Both proton pumps catalyze electrogenic H^+-translocation to generate inside-acidic and inside-positive electrochemical potential for secondary transport of many metabolites [1–3]. Vacuolar H^+-ATPase has been subjected to extensive studies, while vacuolar H^+-PPase is currently recognized as a distinct type of ion translocator [1–3]. Vacuolar H^+-PPase has been successfully purified from various sources and was shown as a homodimer consisting of a single polypeptide with a calculated molecular mass of 71–80 kDa [2,4–7]. Recently, several essential amino acid residues involved in the enzymatic reaction of vacuolar H^+-PPase were determined [7–13]. For instance, a putative substrate binding motif of DX_7KXE on loop *e* and acidic DX_3DX_3D motifs on both loops *e* and *m* of cytosolic side have been proposed, respectively [14,15]. Furthermore, the PP_i hydrolytic activity of vacuolar H^+-PPase was markedly decreased in a concentration-dependent manner by fluorescein 5′-isothiocyanate (FITC), indicating the involvement of a lysine residue in enzymatic reactions [12]. Notwithstanding, other essential regions and residues in vacuolar H^+-PPase for the enzymatic function, proton translocation, and ligand binding still require further elucidation.

Interaction between dimeric subunits of vacuolar H^+-PPase has also been studied previously [11,16,17]. Radiation inactivation analysis demonstrated that dimeric structure of vacuolar H^+-PPase on tonoplastic membrane is

Abbreviations: DSC, differential scanning calorimetry; FITC, fluorescein 5′-isothiocyanate; PPase, pyrophosphatase

* Corresponding author. Tel./fax: +886-3-5742688.
E-mail address: rlpan@life.nthu.edu.tw (R.L. Pan).

0005-2728/$ - see front matter © 2004 Elsevier B.V. All rights reserved.
doi:10.1016/j.bbabio.2004.02.001

required for both enzymatic activity and PP_i-supported proton translocation [16]. Further target size measurement revealed that only one subunit of the purified dimeric complex would sufficiently display enzymatic reaction of vacuolar H^+-PPase [16]. Moreover, high hydrostatic pressure was employed to inhibit vacuolar H^+-PPase through subunit dissociation of the enzyme from an active into inactive form [17]. The physiological substrate and its analogues enhance the high-pressure inhibition of vacuolar H^+-PPase. These lines of evidence indicate explicitly the importance of protein–protein interaction for this novel proton translocating enzyme and suggest a notion that association of identical subunits of vacuolar H^+-PPase is not random but proceeds by a specific manner [17]. In spite of these reports, the relationship between structure and function of this homodimeric protein complex still requires further extensive studies.

Thermoinactivation analysis is a powerful tool to examine protein structure, subunit interaction, and structural stability of many enzymes [18–20]. It has been also used to study effects of different ligands on structure and function of macromolecules [19,21–23]. In this report, thermoinactivation technique was employed to investigate the heat susceptibility of vacuolar H^+-PPase in the presence and absence of ligands (substrate and inhibitors). A working model is thus proposed to interpret the subunit-subunit interaction of vacuolar H^+-PPase as determined by thermal response of the enzyme.

2. Materials and methods

2.1. Plant materials

Hypocotyl tissues of 4-day-old etiolated mung bean (*Vigna radiata* L.) seedlings were harvested, excised, chilled on ice, and then used as starting plant materials.

2.2. Preparation of tonoplast and vacuolar H^+-PPase

Tonoplast vesicles of high purity were prepared as previously described [6,12]. Vacuolar H^+-PPase was purified from tonoplast membrane by methods modified from those of Maeshima and Yoshida [6] and Britten et al. [4].

2.3. Enzyme assay and protein determination

PPase activities were determined by measuring the release of P_i from PP_i. Aliquots of purified vacuolar H^+-PPase (2–5 μg) were assayed in a 1.0-ml reaction medium containing 25 mM Mops/KOH (pH 7.2), 1 mM $MgSO_4$, 1 mM K_4PP_i, 50 mM KCl, 80 μg/ml phosphatidylcholine (soybean, type IV-S), 0.01% (w/v) Triton X-100 at 33 °C for 15 min. After incubation, the reaction was terminated by adding a solution containing 1.7% (w/v) ammonium molybdate, 2% (w/v) SDS, and 0.02% (w/v) 1-amino-2-naphthol-4-sulfonic acid. The released P_i was determined spectrophotometrically as described elsewhere [12,24,25].

Protein concentration was measured by a modified Lowry method [26] or the dye-binding method of Bradford [27] with BSA as a standard.

2.4. Thermal inactivation

Vacuolar H^+-PPase (5 μg) was incubated at various temperatures for 10 min in a medium of 50 mM Tris/HCl (pH 7.2), 50 mM KCl, and 1 mM DTT. Thermal treatments of the enzyme were then terminated by removal of aliquots into an appropriate assay solution at 33 °C. Enzymatic activities and fluorescence were measured as indicated above and in following sections.

Parameters of thermal inactivation were obtained from the relationship as follows:

$$\Delta G^{\neq} = -RT \ln(k_{in}h/k_bT)$$

$$k_{in} = Ae^{-E_a/RT}$$

where h is the Planck constant (6.626×10^{-34} J·s), R is the gas constant (8.31 J/mol·K), k_b is the Boltzmann constant (1.38×10^{-23} J/K), A is the frequency factor, E_a is the activation energy, T is the temperature at which reactions measured, and k_{in} is the apparent rate constant of the thermal inactivation, determined from the first order rate kinetics. An Arrhenius plot of the rate of inactivation was used to yield the activation energy (E_a) and the constant A.

2.5. FITC labeling

Purified vacuolar H^+-PPase was incubated with 0.5 mM FITC in a medium containing 50 mM Mops/KOH (pH 7.5), and 20% (v/v) glycerol at 33 °C for 10 min. After labeling, the reaction was stopped and free FITC removed by passing through Sephadex G-25 column pre-equilibrated with the same buffer. The FITC-labeled vacuolar H^+-PPase was used immediately or stored at −70 °C for further studies.

2.6. Spectroscopic measurements

Spectra of proteins were examined in a medium of 50 mM Tris/HCl (pH 7.2), 50 mM KCl, and 1 mM DTT. Intrinsic fluorescence measurement of vacuolar H^+-PPase was carried out with excitation wavelengths at 275 nm and emission wavelength at 304, respectively, using an SLM 4800 fluorescence spectrometer. Secondary structure of vacuolar H^+-PPase (2.5 μM) was determined by circular dichroism (CD) at various temperatures on a Lakewoods N.J. Model 62A DS spectrometer [17]. CD spectra shown were averages of three scans for each sample.

2.7. Differential scanning calorimetry (DSC)

DSC was performed with a Seiko Microcalorimeter (Seiko Instruments Inc., Japan). Samples (6 mg/ml) were incubated at about 4 °C in a buffer containing 50 mM Tris/HCl (pH 7.2), 50 mM KCl, and 1 mM DTT after loading the cells. The same volume of buffer was used in the reference cell, and the cooling box was purged with liquid nitrogen. Data were collected from 4 to 100 °C at a scan rate of 1 °C/min.

2.8. Chemicals

FITC was purchased from Sigma (St. Louis, MO, USA) and PP_i from Merck (Damstadt, Germany). All other chemicals were of the highest analytic grade and used without further purification.

3. Results

3.1. Temperature dependence of PP_i hydrolysis

Before thermal treatment of vacuolar H^+-PPase, the purity and molecular size of native protein were determined. According to our routine purification procedure, a highly purified preparation was obtained, of which only one band (73 kDa) was visualized on SDS-PAGE pattern (Fig. 1). The impurity contamination was almost negligible in the preparation. The purified vacuolar H^+-PPase was then subjected to size exclusion gel filtration chromatography and yielded a single peak (data not shown; cf. Refs. [12,16]). The molecular mass is approximately 145 kDa for the native enzyme, confirming the purified vacuolar H^+-PPase from tonoplast of mung bean is a homodimer [16]. We are thus convinced that our routinely purified enzyme was suitable for this study. Furthermore, we used FITC as lysine-specific modifier to probe the structure of the active domain of vacuolar H^+-PPase. FITC could inhibit vacuolar H^+-PPase progressively with an I_{50} value, the concentration at which half of control enzymatic activity was obtained, occurring at 0.5 mM [12]. Under this condition, only one subunit of the homodimeric vacuolar H^+-PPase was labeled [12].

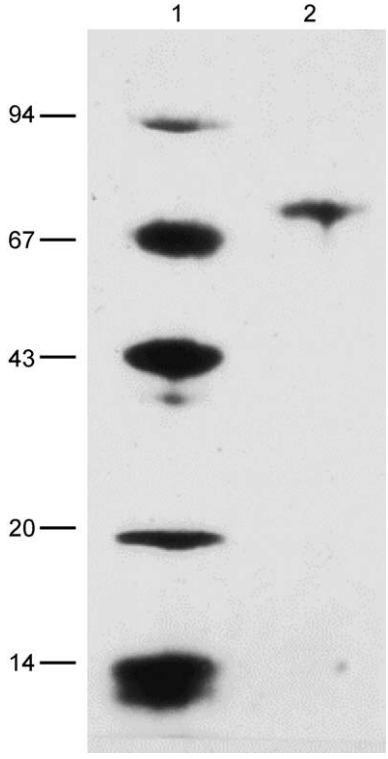

Fig. 1. SDS-PAGE of purified vacuolar H^+-PPase from etiolated mung bean. Mung bean vacuolar H^+-PPase was purified and subjected to SDS-PAGE as described previously [12]. Lane 1, standard markers with molecular mass indicated on the left; lane 2, purified vacuolar H^+-PPase.

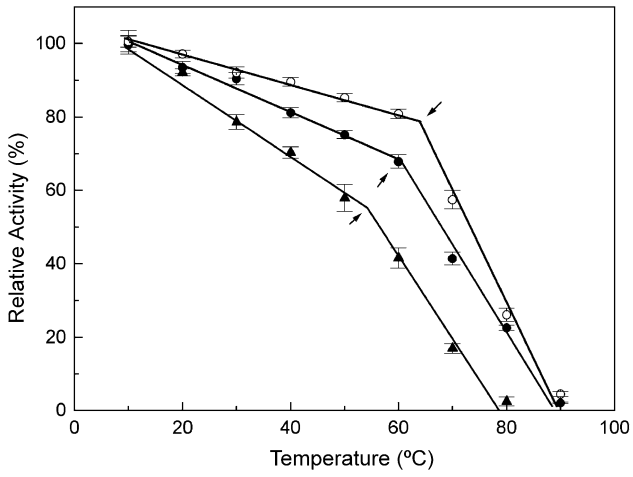

Fig. 2. Temperature effects on the enzymatic activities of vacuolar H^+-PPases. Purified vacuolar H^+-PPase (5 μg) was incubated at various temperatures for 10 min. After the thermal treatment, PP_i hydrolysis activities of enzymes were assayed. (●) Control vacuolar H^+-PPase; (○) vacuolar H^+-PPase in the presence of $Mg^{2+}PP_i$; (▲) FITC-labeled H^+-PPase.

To observe thermal effects on vacuolar H^+-PPase, three types of the enzyme, such as control, substrate ($Mg^{2+}PP_i$)-bound, and FITC-labeled H^+-PPases, were pretreated for 10 min at temperatures of a wide range from 10 to 90 °C and then activities accordingly measured at 33 °C (Fig. 2). As the pretreatment temperature increased, the PP_i hydrolysis activities of the three types of vacuolar H^+-PPase were significantly declined in progressive manners. PPase activities of each type were temperature-dependent and respectively exhibited two phases at different transition temperatures (T_m). It is obvious that the vacuolar H^+-PPase might undergo a structural change upon thermal treatment, resulting in the loss of enzymatic activity. The transition temperature between two phases of control vacuolar H^+-PPase occurs at about 60 °C. Furthermore, the T_m values of substrate-bound and FITC-labeled vacuolar H^+-PPases were approximately at 67 and 53 °C, respectively. These results suggested explicitly that the substrate ($Mg^{2+}PP_i$) of vacuolar H^+-PPase provides protection against thermal inactivation

and increases its phase transition temperature. In contrast, half-inhibited vacuolar H^+-PPase (with only one subunit of homodimer modified by FITC) is more fragile to thermal treatment and possesses lower transition temperature.

3.2. Temperature effects on spectral properties of H^+-PPase

In parallel experiments, intrinsic fluorescence at 304 nm was measured using control, $Mg^{2+}PP_i$-bound, and FITC-labeled PPases (Fig. 3). Each type of enzyme preparations also displays two phases of structure as suggested from the plots of intrinsic fluorescence versus temperature. The order of transition temperature was also $Mg^{2+}PP_i$-bound> control>FITC-labeled PPases, coincident with that determined from decline of respective specific activities (cf. Fig. 2). These data confirm the above speculation that the vacuolar H^+-PPase might undergo a change in conformational state at the transition temperature, resulting in a decrease in enzymatic activity. It is likely that distinct conformational states alter the behavior of intrinsic fluorescence of amino acid residues observed. The different transition temperature implies clearly that $Mg^{2+}PP_i$-incorporated and FITC-labeled PPases possessed distinct modes of susceptibility and exhibited different structure from control H^+-PPase.

Secondary structure of vacuolar H^+-PPase was further investigated using CD spectroscope at different temperatures (Fig. 4). The CD spectra of vacuolar H^+-PPase were scanned from wavelength 190 to 260 nm at temperatures from 25 to 80 °C and the relative α-helix contents were calculated from ellipticity at 210 and 224 nm [28,29].

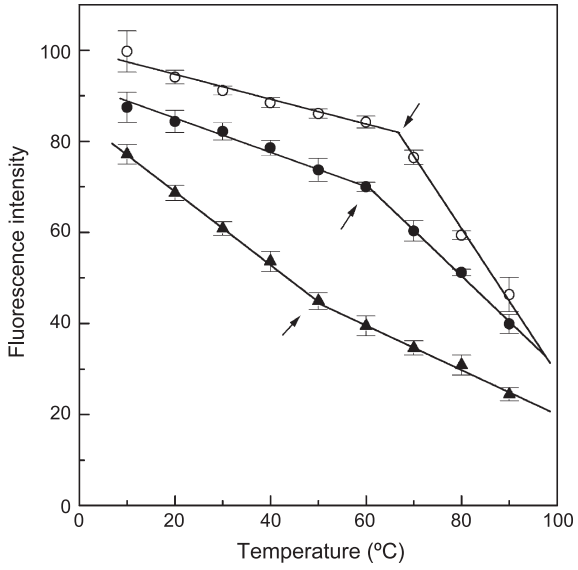

Fig. 3. Temperature dependence of intrinsic fluorescence of vacuolar H^+-PPases. Purified vacuolar H^+-PPase (5 μg) was incubated at various temperatures for 10 min. After the thermal treatment, the fluorescence intensity of vacuolar H^+-PPase at 304 nm was measured. The excitation wavelength was 275 nm. (●) Control vacuolar H^+-PPase; (○) vacuolar H^+-PPase in the presence of $Mg^{2+}PP_i$; (▲) FITC-labeled H^+-PPase.

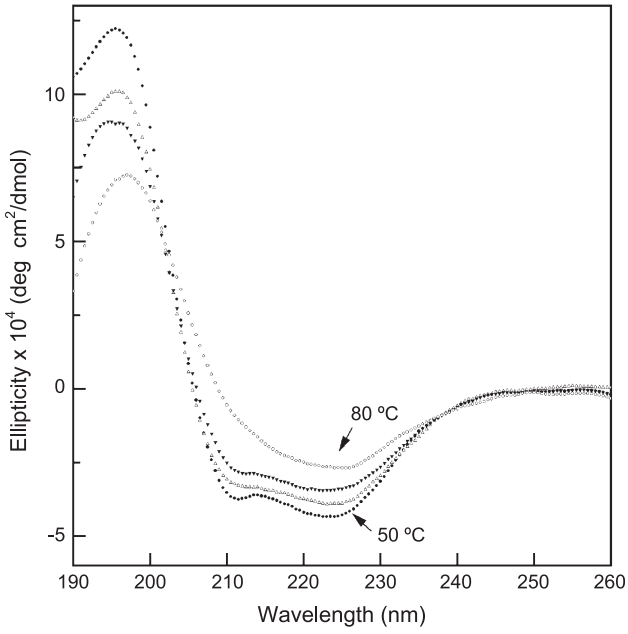

Fig. 4. Temperature effect on the secondary structure of vacuolar H^+-PPase. Secondary structure of purified vacuolar H^+-PPase (2.5 μM) was determined by CD at various temperatures. Spectra from bottom to top are at 50, 60, 70, and 80 °C, respectively. Each data point of the spectra was the average of three scans. The CD spectra and α-helix content do not show any significant change at temperatures from 25 to 50 °C, while a great variation above 50 °C was observed. (●) 50 °C; (△) 60 °C; (▼), 70 °C; (○), 80 °C. The α-helix contents were accordingly calculated [28,29] as 58.7%, 51.2%, 45.6%, and 34.1%, respectively.

Since the presence of Mg^{2+} and FITC moiety could interfere the measurement of CD spectra, only that of control vacuolar H^+-PPase was determined. The CD spectra and α-helix content of purified vacuolar H^+-PPase do not show any significant change at temperatures from 25 to 50 °C (Fig. 4, -●-), while a great variation above 50 °C was observed (cf., Fig. 4, -Δ-, -▼-, and -○-). An α-helix content of 58.7% was obtained accordingly for vacuolar H^+-PPase at temperatures from 25 to 50 °C. As temperature increased, the CD spectra significantly became less intense and characteristic troughs at 210 and 224 nm gradually disappeared. The α-helix contents of 51.2%, 45.6%, and 34.1% were calculated for vacuolar H^+-PPase at temperatures of 60, 70 and 80 °C, respectively. These results unambiguously indicate that a significant state transition of vacuolar H^+-PPase and consequently a conformational change of the enzyme occur at T_m, yielding a decline in α-helix content.

3.3. Kinetic analysis of thermal inactivation

High temperature induced rapid inactivation of control, $Mg^{2+}PP_i$-bound, and FITC-labeled PPases in a time-dependent manner (Fig. 5). The rate constants (k_{in}) of inactivation at the elevated temperature were obtained from the plots of ln(activity) versus time of heat incubation and summarized in Table 1. Compared to control H^+-PPase,

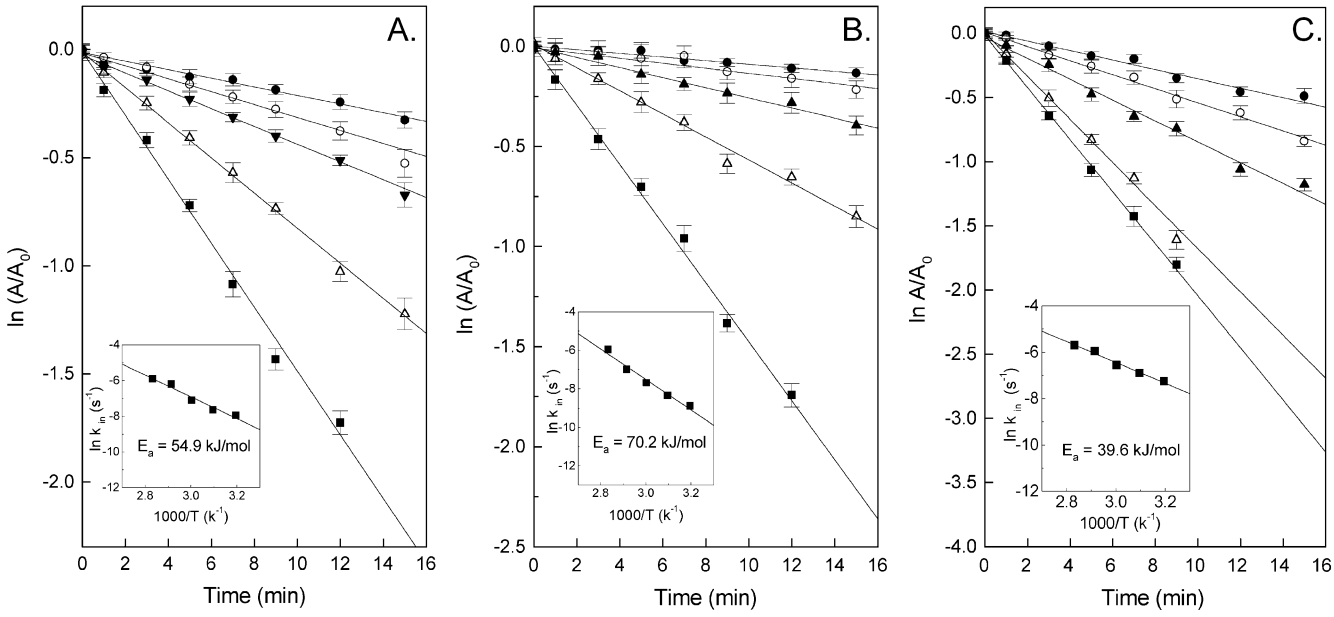

Fig. 5. Time course of thermoinactivation for vacuolar H^+-PPases. Time courses of thermoinactivation for control (A), $Mg^{2+}PP_i$-bound (B), and FITC-labeled (C) vacuolar H^+-PPases, respectively. Treatment and assay conditions were as described under Materials and methods. Vacuolar H^+-PPase (5 μg) of each type was incubated at various temperatures: (●) 313 K, (○) 323 K, (▼) 333 K, (△) 343 K, and (■) 353 K. Inserts: Arrhenius plots for thermoinactivation. The values of rate constants (k_{in}) were determined according to the first-order rate kinetics: $\ln(A/A_0) = -k_{in}t$. The values of activation energy (E_a) for different preparations were obtained from: $k_{in} = Ae^{-E_a/RT}$ as described under Materials and methods.

substrate-bound enzyme showed a decrease in the rate constant (k_{in}) of thermal inactivation. In other words, the presence of physiological substrate promotes thermostability of vacuolar H^+-PPase. In contrast, FITC-labeling decreases the thermo-tolerance of vacuolar H^+-PPase as determined by the increase in the k_{in} values. Furthermore, Arrhenius plots of thermal inactivation were used to measure the activation energy (E_a) of vacuolar H^+-PPase (Fig. 5, inserts). The thermodynamic parameters thus obtained of each type of vacuolar H^+-PPase were summarized in Table 2. Vacuolar H^+-PPase in the presence of physiological substrate displayed relatively higher energy barrier (70.2 kJ/mol) than control enzyme (54.9 kJ/mol) and that labeled by FITC (39.6 kJ/mol). Obviously, FITC-labeled PPase showed a considerably higher thermosensitivity upon heat treatment. In contrast, vacuolar H^+-PPase could be stabilized and its tolerance to high temperature could be elevated by its physiological substrate $Mg^{2+}PP_i$. The free energy ($\Delta G^{\neq}$) and other thermodynamic parameters ($\Delta H^{\neq}$ and $\Delta S^{\neq}$) for thermoinactivation for control, substrate-bound, and FITC-modified vacuolar H^+-PPases were calculated and also summarized in Tables 1 and 2, respectively. Comparing the thermodynamic parameters, we suggest that vacuolar H^+-PPase possesses two temperature-dependent conformational states and probably undergoes a conformational change as the temperature shifts. It is also conceivable that physiological substrate ($Mg^{2+}PP_i$) could stabilize the structure and function of vacuolar H^+-PPase against heat inactivation.

Table 1
Apparent rate constants (k_{in}) of thermoinactivation and free energy ($\Delta G^{\neq}$) at different temperatures

Enzymes	Temperature (K)	k_{in} ($\times 10^{-4}$ s^{-1})	$\Delta G^{\neq}$ (kcal/mol)
Control PPase	313	3.5	23.3
	323	4.8	23.9
	333	8.3	24.3
	343	20.3	24.4
	353	27.4	24.9
$Mg^{2+}PP_i$-PPase	313	1.6	23.8
	323	2.4	24.3
	333	4.6	24.7
	343	9.2	25.0
	353	25.7	25.0
FITC-PPase	313	7.0	22.9
	323	10.1	23.4
	333	14.1	23.9
	343	26.1	24.2
	353	33.5	24.8

The values of k_{in} were obtained from the time course of heat inactivation (Fig. 5); $\Delta G^{\neq}$ was calculated from the relationship $\Delta G^{\neq} = -RT\ln(k_{in}h/k_bT)$, where h is the Planck constant, R and k_b are the gas constant and Boltzmann constant, respectively.

Table 2
Parameters of the thermoinactivation for vacuolar H^+-PPases

Enzymes	T_M (K)	E_a (kJ/mol)	$\Delta H^{\neq}$ (kJ/mol)	$\Delta S^{\neq}$ (− cal/mol K)
Control PPase	331.1	54.9	48.3	37.6
$Mg^{2+}PP_i$-PPase	334.2	70.2	59.8	30.4
FITC-PPase	326.1	39.6	35.4	46.1

Values of E_a and T_M were calculated from Arrhenius plots (Fig. 5, inserts) and Fig. 6, respectively. The calculated energy of activation, $\Delta H^{\neq}$ and $\Delta S^{\neq}$ were obtained from the equation: $\Delta G^{\neq} = \Delta H^{\neq} - T\Delta S^{\neq}$.

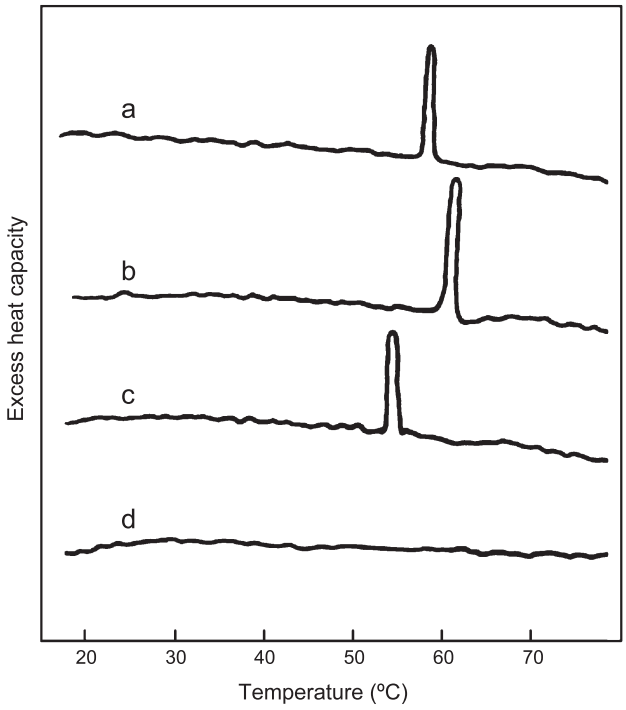

Fig. 6. DSC profiles of vacuolar H^+-PPases. Various types of H^+-PPase (6 mg/ml) were incubated at 4 °C for 10 min and the DSC trace measured. The melting temperatures (T_M) on DSC were 58.1, 61.2, and 53.1 °C for (a) control, (b) $Mg^{2+}PP_i$-bound, and (c) FITC-labeled PPases, respectively. (d) Second scan of the same sample after denaturation of proteins. The scan rates for all traces were 1 °C/min.

3.4. DSC of the vacuolar H^+-PPase

Highly sensitive DSC has been employed as a useful tool in the study of the structure and phase behavior of biological membranes and macromolecules [18,19,30]. To further verify the role of the substrate and the modifier in the structural stability of enzyme, control, $Mg^{2+}PP_i$-bound, and FITC-labeled H^+-PPases were subjected to DSC (Fig. 6). Obvious differences in the melting temperature (T_M) for these three types of the enzyme on DSC were observed. The T_M values were 331.1, 334.2, and 326.1 K for control, $Mg^{2+}PP_i$-bound, and FITC-labeled H^+-PPases, respectively. $Mg^{2+}PP_i$ did protect the enzyme from heat-induced phase transition, thus shifting the T_M value of $Mg^{2+}PP_i$-bound H^+-PPase to relatively higher temperature than control H^+-PPase. In contrast, the FITC-labeled H^+-PPase exhibited the lowest T_M value. Notwithstanding, the hysteric scanning of heat treatment demonstrates that the state transition of H^+-PPase induced by heat is irreversible (Fig. 6d).

4. Discussion

The enzymatic activity of purified vacuolar H^+-PPase could be inhibited by heat treatment in a temperature- and time-dependent manner. The slope of inhibition curve is drastically changed at a temperature above 60 °C. The biphasic curve strongly suggests that vacuolar H^+-PPase possesses two possible structural states upon the heat treatment. This possibility is also confirmed by the spectral analysis of purified vacuolar H^+-PPase following thermal inactivation. Intrinsic fluorescence changes indicate the conformational drift of purified vacuolar H^+-PPase after heat treatment. CD analysis also demonstrated the loss of α-helix structure of purified vacuolar H^+-PPase upon heat treatment. Furthermore, DSC profile showed an obvious change of heat capacity of purified vacuolar H^+-PPase along heat scanning. All these data suggest explicitly the existence of two states of purified vacuolar H^+-PPase. Taking this line of evidence into account, we thus speculate that the enzyme state (S_1) of vacuolar H^+-PPase at temperature below T_m is more thermoresistant, while the state at temperature above T_m (S_2) is more susceptible to thermoinactivation.

Moreover, $Mg^{2+}PP_i$-incorporated and FITC-labeled PPases also exhibit two phases of structure as determined from the plots of activity inhibition and intrinsic fluorescence versus temperature. Different transition temperatures suggest that $Mg^{2+}PP_i$-incorporated and FITC-labeled PPases possessed different susceptibilities to heat treatment and presented distinct structures from native vacuolar H^+-PPase. As for $Mg^{2+}PP_i$-bound H^+-PPase, the T_m value is higher than its native form, indicating that the intercalation of substrate ($Mg^{2+}PP_i$) in the active site of vacuolar H^+-PPase consequently brings the enzyme to a state more resistant to heat treatment. The Arrhenius analysis also showed a higher energy barrier for $Mg^{2+}PP_i$-bound H^+-PPase than native enzyme, confirming the role of the substrate to stabilize native vacuolar H^+-PPase. The protection of substrates against thermoinactivation was also frequently observed for many enzymes [31]. In contrast, it is

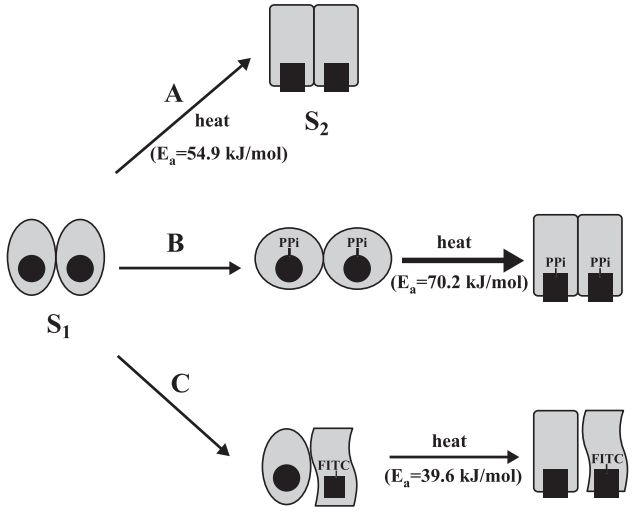

Fig. 7. Working model for heat-induced conformational changes of vacuolar H^+-PPases. Heat-induced conformational change of: (A) control vacuolar H^+-PPase; (B) vacuolar H^+-PPase in the presence of substrate; (C) FITC-labeled vacuolar H^+-PPase. The stoichiometry of labeling was 1.0 mol FITC/mol PPase.

well known that vacuolar H^+-ATPase, another type of proton pumping enzyme on the same vacuolar membrane, is a cold-labile protein complex [32]. The presence of its physiological substrate, Mg^{2+}-ATP, could enhance cold-inactivation of vacuolar H^+-ATPase. From this viewpoint, we believe that the protection of the physiological substrate of vacuolar H^+-PPase may offer an advantage for vacuoles to regulate its proton pumping efficiency against surrounding temperature variations.

Notwithstanding, FITC modification makes vacuolar H^+-PPase more vulnerable to heat inactivation, since both T_m and E_a values are lower than native enzyme. Furthermore, the transition from lower temperature state to higher temperature state of FITC-PPase is not as obvious as those of substrate-bound and native vacuolar H^+-PPase, when comparing the changes of slopes among these curves (cf., Figs. 2 and 3). This difference might be due to the fact that one of the catalytic sites of homodimeric H^+-PPase was occupied by FITC moiety, resulting in the change of subunit–subunit interaction of the enzyme complex. The energy barrier for changing from one state to another is smoothed. In our previous study, we demonstrated FITC could inhibit this vacuolar H^+-PPase progressively with an I_{50} value occurring at 0.5 mM [12]. The stoichiometry of labeling at this concentration was 1.0 mol FITC/mol PPase; that is, only one subunit of the homodimeric vacuolar H^+-PPase was modified [12]. Alternatively, the possibility that both subunits of half of enzyme population were labeled by FITC is excluded, since the modification decreases the K_m of H^+-PPase but leaves its V_{max} unchanged [12]. We thus speculate that modification by FITC changes the subunit–subunit interaction of vacuolar H^+-PPase complex, consequently smoothing the energy barrier between two states.

Taken together, a working model is proposed for the phenomenon observed above (Fig. 7). The vacuolar H^+-PPase functions as a homodimer (S_1 state) during PP_i hydrolysis as determined by gel filtration and radiation inactivation [16,17]. High temperature might induce a conformational change (S_2 state) of the vacuolar H^+-PPase, making PP_i more accessible to the active site ($E_a = 54.9$ kJ/mol; pathway A). On the other hand, the intercalation of substrate ($Mg^{2+}PP_i$) in the active site of vacuolar H^+-PPase consequently strengthens the structure of the enzyme, thereby resulting in high resistance to heat (pathway B). Comparing the activation parameters, we suggested that the physiological substrate ($Mg^{2+}PP_i$) could stabilize the structure and activity of heat inactivation as determined by higher energy barrier ($E_a = 70.2$ kJ/mol). Furthermore, FITC, labeling an essential lysine in the active domain of vacuolar H^+-PPase, modifies the subunit–subunit interaction of the enzyme, bringing the enzyme to a state more vulnerable to heat treatment ($E_a = 39.6$ kJ/mol; pathway C). Conceivably, the subunit–subunit interaction in homodimeric H^+-PPase plays an important role in maintaining the functional structure of this novel vacuolar proton-pumping enzyme.

Acknowledgements

This work was supported by the grant from National Science Council, Republic of China (NSC 91-2311-B-007-035) to RLP.

References

[1] T. Nishi, M. Forgac, The vacuolar H^+-ATPases—nature's most versatile proton pumps, Nat. Rev., Mol. Cell Biol. 3 (2002) 94–103.
[2] M. Maeshima, Vacuolar H^+-pyrophosphatase, Biochim. Biophys. Acta 1465 (2000) 37–51.
[3] M. Maeshima, Tonoplast transporters: organization and function, Annu. Rev. Plant Physiol. Plant Mol. Biol. 52 (2001) 469–497.
[4] C.J. Britten, J.C. Turner, P.A. Rea, Identification and purification of substrate-binding subunit of higher plant H^+-translocating inorganic pyrophosphatases, FEBS Lett. 256 (1989) 200–206.
[5] V. Sarafian, R.J. Poole, Purification of an H^+-translocating inorganic pyrophosphatases from vacuole membranes of red beet, Plant Physiol. 91 (1989) 34–38.
[6] M. Maeshima, S. Yoshida, Purification and properties of vacuolar membrane proton-translocating inorganic pyrophosphatase from mung bean, J. Biol. Chem. 264 (1989) 20068–20073.
[7] S.J. Yang, S.S. Jiang, C.M. Tzeng, S.Y. Kuo, S.H. Hung, R.L. Pan, Involvement of tyrosine residue in the inhibition of plant vacuolar H^+-pyrophosphatase by tetranitromethane, Biochim. Biophys. Acta 1294 (1996) 89–97.
[8] S.Y. Kuo, R.L. Pan, An essential arginyl residue in the tonoplst pyrophosphatase from etiolated mung bean seedlings, Plant Physiol. 93 (1990) 1128–1133.
[9] R.-G. Zhen, E.J. Kim, P.A. Rea, Localization of cytosolically oriented maleimide-reactive domain of vacuolar H^+-pyrophosphatase, J. Biol. Chem. 269 (1994) 23342–23350.
[10] R.-G. Zhen, E.J. Kim, P.A. Rea, Acidic residues necessary for pyrophosphate-energized pumping and inhibition of the vacuolar H^+-pyrophosphatase by *N*,*N*′-dicyclohexylcarbodiimide, J. Biol. Chem. 272 (1997) 22340–22348.
[11] S.J. Yang, S.S. Jiang, S.Y. Kuo, S.H. Hung, M.F. Tam, R.L. Pan, Localization of a carboxylic residue possibly involved in the inhibition of vacuolar H^+-pyrophosphatase by *N*,*N*′-dicyclohexylcarbodiimide, Biochem. J. 342 (1999) 641–646.
[12] S.J. Yang, S.S. Jiang, R.C. Van, Y.Y. Hsiao, R.L. Pan, A lysine residue involved in the inhibition of vacuolar H^+-pyrophosphatase by fluorescein 5′-isothiocyanate, Biochim. Biophys. Acta 1460 (2000) 375–383.
[13] Y.Y. Hsiao, R.C. Van, H.H. Hung, R.L. Pan, Diethylpyrocarbonate inhibition of vacuolar H^+-pyrophosphatase possibly involves a histidine residue, J. Protein Chem. 21 (2002) 51–58.
[14] Y. Nakanishi, T. Saijo, Y. Wada, M.J. Maeshima, Mutagenic analysis of functional residues in putative substrate-binding site and acidic domains of vacuolar H^+-pyrophosphatase, J. Biol. Chem. 276 (2001) 7654–7660.
[15] M. Baltscheffsky, A. Schultz, H. Baltscheffsky, H^+-PPases: a tightly membrane-bound family, FEBS Lett. 457 (1999) 527–533.
[16] C.M. Tzeng, C.Y. Yang, S.J. Yang, S.S. Jiang, S.Y. Kuo, S.H. Hung, J.T. Ma, R.L. Pan, Subunit structure of vacuolar proton-pyrophosphatase as determined by radiation inactivation, Biochem. J. 316 (1996) 143–147.
[17] S.J. Yang, S.J. Ko, Y.R. Tsai, S.S. Jiang, S.Y. Kuo, S.H. Hung, R.L. Pan, Subunit interaction of vacuolar H^+-pyrophosphatase as determined by high hydrostatic pressure, Biochem. J. 331 (1998) 395–402.
[18] K.E. Hightower, R.E. McCarty, Structural stability of chloroplast coupling factor 1 determined by differential scanning calorimetry and cold inactivation, Biochemistry 35 (1996) 4852–4857.

[19] C. Anteneodo, A.M. Rodahl, E. Meiering, M.L. Heynen, G.A. Sennisterra, J.R. Lepock, Interaction of dibucaine with the transmembrane domain of the Ca^{2+}-ATPase of sarcoplasmic reticulum, Biochemistry 33 (1994) 12283–12290.
[20] J.F. Brandts, L.N. Lin, Study of strong to ultratight protein interactions using differential scanning calorimetry, Biochemistry 29 (1990) 6927–6940.
[21] T.J. Ahern, A.M. Klibanov, Analysis of processes causing thermal inactivation of enzymes, Methods Biochem. Anal. 33 (1988) 91–127.
[22] O. Munch, D. Tritsch, Irreversible thermoinactivation of glucoamylase from *Aspergillus niger* and thermostabilization by chemical modification of carboxyl groups, Biochim. Biophys. Acta 1041 (1990) 111–116.
[23] U. Arnold, R. Ulbrich-Hofmann, Kinetic and thermodynamic thermal stabilities of ribonuclease A and ribonuclease B, Biochemistry 36 (1997) 2166–2172.
[24] C.H. Fiske, Y. Subbarow, The colorimetric determination of phosphorous, J. Biol. Chem. 66 (1925) 378–400.
[25] M.Y. Wang, Y.H. Lin, W.M. Chow, T.P. Chung, R.L. Pan, Purification and characterization of tonoplast H^+-ATPase from etiolated mung bean seedlings, Plant Physiol. 90 (1989) 475–481.
[26] E. Larson, B. Howlett, A.T. Jagendorf, Artificial reductant enhancement of the Lowry method for protein determination, Anal. Biochem. 155 (1986) 243–248.
[27] M.H. Bradford, Rapid and sensitive method for the microgram quantities of protein utilizing the principle of protein-dye binding, Anal. Biochem. 72 (1976) 248–254.
[28] P.J. Gans, P.C. Lyu, M.C. Manning, R.W. Woody, N.R. Kallenbach, The helix-coil transition in heterogeneous peptides with specific side-chain interactions: theory and comparison with CD spectral data, Biopolymers 31 (1991) 1605–1614.
[29] R.S. Mani, E.V. Usova, S. Eriksson, C.E. Cass, Hydrodynamic and spectroscopic studies of substrate binding to human recombinant deoxycytidine kinase, Nucleosides Nucleotides Nucleic Acids 22 (2003) 175–192.
[30] P.E. Morin, E. Freire, Direct calorimetric analysis of the enzymatic activity of yeast cytochrome *c* oxidase, Biochemistry 30 (1991) 8494–8500.
[31] T.T. Waldron, K.P. Murphy, Stabilization of proteins by ligand binding: application to drug screening and determination of unfolding energetics, Biochemistry 42 (2003) 5058–5064.
[32] Y. Moriyama, N. Nelson, Cold inactivation of vacuolar proton-ATPases, J. Biol. Chem. 264 (1989) 3577–3582.